Current Cardiology Reports (2019) 21: 11
https://doi.org/10.1007/s11886-019-1096-x

NUCLEAR CARDIOLOGY (V DILSIZIAN, SECTION EDITOR)

Quantification of PET Myocardial Blood Flow

Matthieu Pelletier-Galarneau[1,2] · Patrick Martineau[1,3] · Georges El Fakhri[1]

Published online: 28 February 2019

Abstract

Purpose of Review The aim of this review is to provide an update on quantification of myocardial blood flow (MBF) with positron emission tomography (PET) imaging. Technical and clinical aspects of flow quantification with PET are reviewed.

Recent Findings The diagnostic and prognostic values of myocardial flow quantification have been established in numerous studies and in various populations. MBF quantification has also shown itself to be particularly useful in the assessment of coronary microvascular dysfunction and in evaluation of cardiac allograft vasculopathy. Overall, myocardial flow reserve (MFR) and hyperemic MBF can lead to improved risk stratification by providing information complementary to that of other markers of disease severity, such as fractional flow reserve.

Summary Flow quantification enhances MPI's ability to detect both significant epicardial disease and microvascular dysfunction. With recent technological and methodological advances, flow quantification with PET is no longer restricted to cyclotron-equipped academic centers.

Keywords Positron emission tomography · Myocardial blood flow · Myocardial flow reserve · Coronary artery disease · Myocardial perfusion imaging

Introduction

Myocardial perfusion imaging (MPI) is a nuclear cardiology test used for the diagnosis and risk stratification of coronary artery disease (CAD) [1]. MPI can be performed with either single-photon emission computed tomography (SPECT) or positron emission tomography (PET). The diagnostic accuracy and prognostic value of SPECT MPI has been extensively validated in numerous large studies in the 1990s and 2000s [2]. Although SPECT MPI has been shown to be both sensitive and specific for the detection of CAD, the modality does suffer from some limitations. First, SPECT MPI typically relies on ^{99m}Tc-labeled tracers, such as ^{99m}Tc-sestamibi and ^{99m}Tc-tetrofosmin. The first pass extraction of these tracers is relatively low, which can lead to underestimation of the severity and extent of ischemic changes [3]. Second, SPECT MPI images can be affected by attenuation artifacts which limit diagnostic accuracy, especially in obese patients and with unexperienced readers [4]. Indeed, the relatively low energy of photons used in SPECT imaging (i.e., ^{99m}Tc ~ 140 keV, ^{201}Tl ~ 62–83 keV) makes them susceptible to soft tissue attenuation, which may mimic perfusion defects and degrade image quality. Finally, because SPECT MPI detects relative perfusion defects, *globally* decreased perfusion secondary to balanced three-vessel disease can be missed [5].

PET offers several distinct advantages which can circumvent the shortcomings of SPECT for MPI. Perhaps the most important of these is the quantification of global and regional myocardial blood flow (MBF). Although flow quantification with PET is often thought of as a recently developed and novel technique, it dates back to the 1960s, preceding the use of SPECT MPI [6]. Availability of affordable SPECT tracers and

This article is part of the Topical Collection on *Nuclear Cardiology*

✉ Georges El Fakhri
elfakhri@pet.mgh.harvard.edu

Matthieu Pelletier-Galarneau
matthieu.pelletier-galarneau@icm-mhi.org

Patrick Martineau
pjmartineau@mgh.harvard.edu

[1] Gordon Center for Medical Imaging, Massachusetts General Hospital and Harvard Medical School, Boston, MA, USA

[2] Department of Medical Imaging, Montreal Heart Institute, Montreal, Quebec, Canada

[3] Department of Radiology, Health Sciences Centre, University of Manitoba, Winnipeg, Manitoba, Canada

cameras made SPECT the modality of choice for MPI in the 1990s and 2000s; however, since that time, there has been an increased availability of PET/CT scanners and tracers, and PET MPI with flow quantification has been revived with the hopes of improving upon the demonstrated successes of SPECT MPI.

MBF Quantification—Technical Aspects

Tracers

Table 1 presents the PET tracers currently used for MBF quantification. Of these, ^{13}N-ammonia (^{13}N-NH_3), ^{15}O-water (^{15}O-H_2O), and ^{18}F-flurpiridaz are cyclotron produced. Both ^{13}N-NH_3 and ^{15}O-H_2O require an on-site cyclotron due to their short half-lives (approximately 10 and 2 min, respectively) while ^{18}F-flurpiridaz, with its 110 min half-life, can be produced at a regional cyclotron facility and delivered to nearby imaging departments. ^{18}F-flurpiridaz is currently in phase III trial for FDA approval and is not yet available for routine clinical use. ^{82}Rb-chloride (^{82}Rb-RbCl) is obtained from a ^{82}Sr-^{82}Rb generator. ^{82}Sr-^{82}Rb generators are expensive but allows nigh unlimited ^{82}Rb-RbCl production for a period of up to 8 weeks [7]. Hence, ^{82}Rb-RbCl can be more cost-effective in centers with higher patient throughput [8]. Of the tracers presented in Table 1, ^{82}Rb-RbCl has the longest mean positron range resulting in the lowest spatial resolution, while the spatial resolution when using ^{18}F-flurpiridaz and ^{13}N-NH_3 is limited by the PET scanner [9]. Finally, ^{82}Rb-RbCl has the lowest first pass extraction fraction, which may lead to reduced accuracy of MBF quantification, especially at high flows, compared to other tracers with higher first pass extraction fractions.

Methods

Generally, assessment of MBF with PET relies on first-pass extraction, requiring a dynamic acquisition obtained at the time of radiotracer infusion. As such, patients must remain under the camera during both the pharmacological stimulation and tracer infusion. For this reason, the use of exercise stress is challenging and usually avoided. Alternate methods not requiring first-pass imaging, thereby facilitating exercise stress, have been proposed. For example, quantification of myocardial retention and standardized uptake value (SUV) has been used to estimate MFR [10]. However, these methods are not well suited for tracers with shorter half-lives and most centers currently rely on first-pass methods. A detailed explanation of the first-pass methods used for MBF quantification is beyond the scope of this article and has been reviewed elsewhere (see [11••, 12••]). Briefly, a left ventricular (LV) chamber time activity curve (TAC) serves as the input function, and a myocardial TAC is fitted with a kinetic model. After correcting for the myocardial tracer extraction fraction and spill-over, tissue tracer extraction can be used to provide MBF measurements. Accuracy of MBF quantification will depend on several factors such as LV segmentation, positioning of input function ROI, scanner sensitivity, and quantification algorithms [11••]. Various software implementations, based on different segmentation algorithms, have been validated and shown to correlate well with each other [13].

Accurate assessment of MBF requires that minimal residual activity from the initial (rest) acquisition is present at time of the second (stress) acquisition. For ^{82}Rb-RbCl and ^{15}O-H_2O, with their very short half-lives of 75 s and 2 min, respectively, a complete rest-stress acquisition can be obtained in 30–45 min [11••]. On the other hand, the use of tracers with longer half-lives is problematic as a delay of up to five half-lives between acquisitions is required. For instance, when using ^{13}N-NH_3, the time between acquisitions is roughly 50 min, requiring two separate cyclotron production cycles in order to complete a rest-stress examination. Due to the relatively lengthy half-life of ^{18}F-flurpiridaz (110 min), the delay period may be inconveniently long for many imaging laboratories. For this reason, techniques have been proposed in order to minimize this delay period. For example, a single-

Table 1 Properties of the different PET tracers available for flow quantification

Tracer	Production	Half-life	Advantages	Disadvantages
^{13}N-NH_3	Cyclotron	10 min	Short positron range High extraction fraction	Onsite cyclotron required
^{15}O-H_2O	Cyclotron	2 min	Rapid rest-stress protocol ~ 100% extraction fraction	High blood pool activity Onsite cyclotron required Not FDA-approved
^{18}F-flurpiridaz	Cyclotron	110 min	High extraction fraction Short positron range No onsite cyclotron required Exercise stress possible	Longer acquisition protocol Not yet available
^{82}Rb-RbCl	Generator	1.27 min	Rapid rest-stress protocol No onsite cyclotron required	Long positron range Low extraction fraction

scan rest-stress protocol allowing rest and stress imaging within 15 min has been proposed and validated in pigs using both ^{13}N-NH_3 and ^{18}F-flurpiridaz [14, 15, 16•]. This protocol is under validation in humans and preliminary data support its accuracy [17]. This shortened protocol allows for complete imaging with ^{13}N-NH_3 using a single cyclotron production run.

Clinical Aspects

In addition to relative perfusion images, regional and global MBF measurements are obtained at both rest and stress, with the difference reflecting the heart's ability to regulate blood flow to different parts of the myocardium in order to meet shifting metabolic demands by altering vascular tone in both epicardial and small vessels. With PET MPI, stress acquisition is typically achieved with pharmacological stimulation using an intravenous infusion of dipyridamole, adenosine, or regadenoson. Although exercise stress is preferred for risk assessment as it provides supplementary information on exercise capacity and prognosis [18], it is only very rarely used with PET, even when patients are able to exercise, for reasons explained above.

Factors Affecting MBF and MFR

MBF is expressed in absolute units of milliliters per minute per gram (mL/min/g) while MFR is a unitless quantity. Normal resting MBF ranges from 0.6 to 1.2 mL/min/g but can vary due to several factors [19–22]. For example, resting MBF might be reduced in patients receiving medical therapy, such as β-blockers. In addition, some medical conditions distinct from CAD are associated with lower resting MBF. In particular, low resting MBF in patients with hypertrophic cardiomyopathy is related to the presence of myocardial fibrosis and is a predictor of poor clinical status [23]. On the other hand, several factors are associated with increased resting MBF. For instance, higher resting flows are observed in females, elderly, and obese patients [24–26]. As well, elevated resting MBF can be observed in the presence of high oxygen demands; as myocardial oxygen extraction is near maximal, even at rest, any increase in oxygen demand must be met by a proportional increase in MBF. Myocardial oxygen demands are therefore intimately coupled with MBF [27]. Hence, increased contractility, heart rate, and/or afterload during resting acquisition will result in augmented rest MBF and reduced MFR. The rate-pressure product (RPP), defined as the product of heart rate and systolic blood pressure, is frequently used as a proxy for myocardial oxygen demand and an adjusted rest MBF can be calculated with the following formula:

$$\text{Adjusted MBF}_{\text{REST}} = \text{MBF} \times \text{RPP}_{\text{REF}}/\text{RPP}_{\text{REST}},$$

where RPP_{REF} represents the population reference resting RPP, typically between 8000 and 9000 mmHg × bpm, and RPP_{REST} represents the resting RPP at time of acquisition. Adjusted MFR is calculated by dividing stress MBF by adjusted resting MBF. Although RPP is routinely used to adjust resting MBF and MFR in many centers, it does have some important limitations, including the fact that it does not account for differences in myocardial contractility, the major determinant of myocardial oxygen consumption [28•].

Stress MBF can be affected by various pathological factors. Notably, stress MBF is reduced in significant epicardial disease and in microvascular dysfunction, representing an impaired ability to increase perfusion to a vascular territory. Also, several non-pathological factors can affect stress MBF, including the stress method used. With exercise stress and hypercapnic stress, MBF increases roughly by a factor of 2 while, with vasodilators such as dipyridamole, adenosine, and regadenoson, it increases three–fourfold [19–22, 29, 30]. Unlike vasodilator stress agents, dobutamine increases MBF by augmenting myocardial oxygen demands, which usually results in slightly higher stress MBF [31]. Reduced MBF and MFR can also be seen following heart transplant. In this case, reduced stress MBF has been attributed to cardiac allograft vasculopathy (CAV, see below), characterized by intimal hyperplasia rather than CAD [32].

Diagnostic Value of Stress MBF and MFR

Incorporating MBF assessment to MPI enhances overall diagnostic performance. Indeed, addition of absolute flow quantification to MPI was shown to improve the ability to detect significant coronary stenosis with both ^{13}N-NH_3 [33–35] and ^{82}Rb-RbCl [36, 37]. Notably, flow quantification improves the ability of MPI to detect severe multivessel disease [34, 36]. Indeed, the inability to increase flow during stress in all territories due to diffuse (or balanced) disease can result in normal-appearing MPI images; however, this would be accompanied by a reduction in global stress MBF and MFR. Although impaired stress MBF and MFR are sensitive markers of CAD, the use of absolute flow quantification is also associated with a mild decrease in specificity for epicardial disease [28•, 36, 37]. This can be explained by different factors including the detection of microvascular disease and suboptimal response to pharmacological stress misinterpreted as significant epicardial disease.

Both MFR and stress MBF can be used to detect significant CAD. On a per lesion basis, several studies showed that stress

MBF is superior to MFR for detecting hemodynamically significant stenosis (≥ 70% or FFR ≤ 0.8) [38–44]. This can be explained, in part, by the fact that MFR is heavily affected by resting MBF which, in turn, is dependent on several non-pathological factors [28•]. On the other hand, global MFR was shown to provide superior prognostic information compared to stress MBF alone, leading to improved risk stratification [45, 46]. As pointed out in a recent joint position paper on the use of flow quantification in PET, the use of MFR rather than of stress MBF is also justified in patients with low resting MBF as they may present decreased stress MBF as well but will remain asymptomatic due to preserved MFR [11••]. Finally, MFR makes myocardial steal—a marker of poor prognosis—more evident [47]. Hence, there is no definite consensus as to which quantitative measure is superior and both MFR and stress MBF should be integrated in the interpretation of MPI studies to reach a better understanding of the disease process.

Prognostic Value of Stress MBF and MFR

Numerous studies have demonstrated the prognostic value of absolute flow quantification in CAD. A severe reduction of stress MBF (< 1.5 mL/min/g) and MFR (< 1.5) is associated with a higher risk of major adverse cardiovascular events (MACE) and death while a preserved MFR is associated with an excellent prognosis [45, 46, 48–50]. MFR was shown to better predict the risks of cardiac death than several other markers, including left ventricular ejection fraction (LVEF) [48, 49]. In general, an MFR cutoff of 2.0 is used with greater values associated with excellent outcomes, while lower values correlate with an increasing risk of MACE. The predictive value of MFR is maintained over several years of follow up—it was suggested that a normal MPI with normal MFR offers a "warranty" period of 3 years during which the risks of MACE and deaths remains very low [50].

The prognostic value of flow quantification was also studied in various specific populations. For example, in diabetic patients, impaired MFR is associated with a sixfold-increased rate of cardiac death [51]. In diabetics, MFR provides additional prognostic information, beyond that of clinical assessment, LV systolic function, and semi-quantitative measurements of ischemia and scar. Interestingly, the risk of cardiac death in diabetic patients with impaired MFR and without history of revascularization or myocardial infarction (MI) is comparable to that of non-diabetic patients with a history of revascularization or MI but with preserved MFR [51]. Similar results were obtained in a population of patients with chronic kidney failure [52, 53•]. The additional prognostic value of flow quantification in these populations is of particular importance given the known shortcomings of conventional relative MPI in these patient groups. Finally, flow quantification was shown to provide incremental prognostic value in various non-ischemic cardiomyopathies in the absence of significant epicardial disease [54–58]. These studies showed that reduced MFR, attributed to microvascular dysfunction, was consistently associated with higher rates of MACE.

Integration of Absolute Flow Quantification in MPI Interpretation

Different cutoff values of stress MBF have been used to detect significant epicardial lesions, ranging from 1.8 to 2.0 mL/min/g [33, 43, 44, 59]. However, there is no universally accepted threshold for MFR or stress MBF that can be used across all populations to confirm the presence of significant epicardial lesions [60]. Due to the numerous intrinsic and extrinsic factors which affect such thresholds, the interpretation of PET MPI studies cannot rely solely on a single cutoff value for MFR or stress MBF. Rather, the quantitative flow information should be incorporated into the overall interpretation of rest and stress perfusion studies. A perfusion defect in a segment conforming to vascular anatomy on relative uptake images associated with a severely reduced regional MFR (< 1.5) or stress MBF (< 1.5 mL/min/g) confirms the presence of a flow limiting epicardial lesion. In the absence of myocardial perfusion defects, a normal global MFR (> 2.0) or global stress MBF (> 2.0 mL/min/g) exclude with a high degree of confidence high-risk CAD (Fig. 1) [11••, 36, 37]. On the other hand, an impaired global MFR (< 1.5) and global stress MBF (< 1.5 mL/min/g), even in absence of defect on relative perfusion images, raises the possibility of extensive epicardial disease. However, not all cases of apparent impaired global stress MBF and MFR bear a poor prognosis. In fact, various factors need to be considered before reporting such a finding. First, it is critical to exclude any possible technical factors, such as inappropriate injection bolus or movement that could lead to erroneous flow quantification. Second, patients with high resting flow can have low-calculated MFR in the presence of normal stress MBF. In these cases, RPP-adjusted MFR, despite its limitations, can be calculated to account for elevated resting flow. Third, a frequent cause of impaired global MFR or stress MBF is suboptimal response to pharmacological stress. For example, patients who consumed caffeine before pharmacological stress testing with adenosine, dipyridamole, or regadenoson might have a blunted hyperemic response. When this is suspected, a repeat study with adequate preparation (caffeine consumption cessation) or with an alternate stress agent such as dobutamine can be considered.

As stated earlier, another cause of impaired global MFR and stress MBF is significant microvascular disease. Although reduced MFR caused by microvascular dysfunction is associated with higher MACE rates, it does not necessarily indicate the presence of significant epicardial disease. When

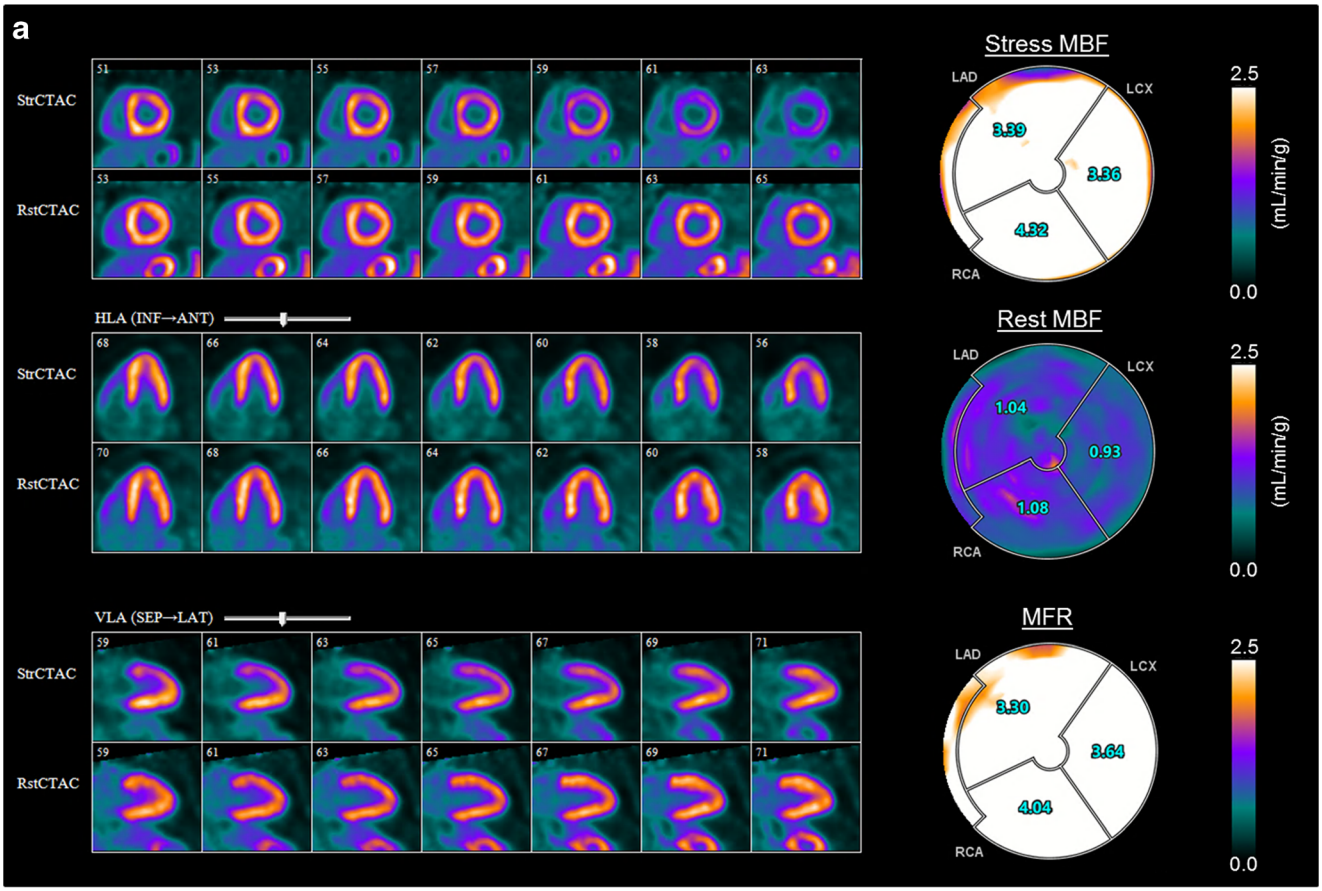

Fig. 1 Relative perfusion images of a ^{82}Rb PET/CT of a 52-year-old male with hypertension, dyslipidemia, significant family history of coronary artery disease, and previous positive treatmill exercise stress test demonstrating a reversible mild perfusion defect involving the anterior wall (**a**). Flow quantification demonstrates a preserve stress MBF (3.4 mL/min/g) and MFR (3.3) in the LAD territory, excluding the presence of significant stenosis. An angiogram performed 3 weeks later (**b**) demonstrates no significant epicardial lesion

extensive epicardial disease causes a global reduction in hyperemic flow, various high risk findings are frequently observed on MPI such as transient ischemic dilatation (TID), right ventricular uptake, reduction of LVEF, and ST changes on ECG (Fig. 2). On the other hand, when microvascular dysfunction causes significant reduction in flow reserve, such findings are usually absent and the patient often report medical conditions associated with microvascular disease such as

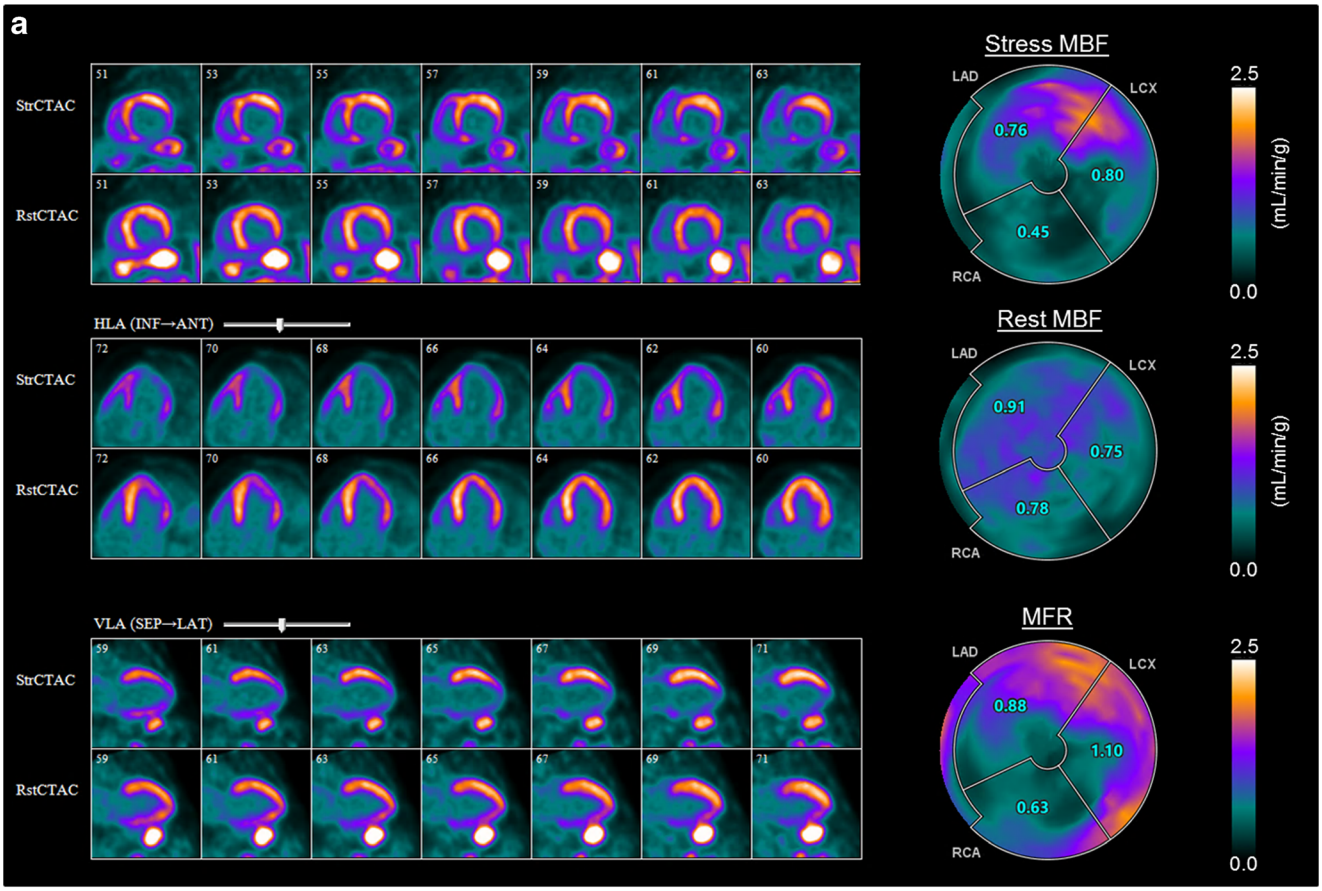

Fig. 2 Images of an asymptomatic 62-year-old male with baseline ECG abnormalities. Relative perfusion images of a ^{82}Rb PET/CT study demonstrate a partially reversible perfusion defect in the inferior-inferolateral territories as well as a reversible, mild perfusion defect involving the anterior wall (**a**). Global MFR was strikingly abnormal at 0.9. Other high risk features including an LVEF drop of 10%, transient ischemic dilatation, and right ventricular uptake are seen. An angiogram performed 1 day later (**b**) demonstrated severe three vessel disease and the patient was referred for coronary bypass surgery

long-standing diabetes, chronic renal failure, prior CABG, or other non-ischemic cardiomyopathy. However, in many cases, differentiating between microvascular dysfunction and extensive epicardial disease can be challenging, if not impossible.

Integrating flow measurements with all available clinical information is critical to reach a comprehensive interpretation of MPI and minimize false positive studies [61, 62].

MFR Vs FFR

Fractional flow reserve (FFR) is a measurement obtained during invasive angiography to evaluate the hemodynamic significance of an epicardial lesion. It is calculated by dividing blood pressure distal to a lesion under pharmacological hyperemia by the pressure proximal to the lesion and conceptually represents the fraction of maximal blood flow going through a stenotic vessel compared to what it would be in absence of stenosis. FFR is used to guide revascularization decisions and a FFR value of 0.8 or greater is often used to exclude a hemodynamically significant lesion [63–65]. Although there is a correlation between MFR and FFR, the two are discordant in 10 to 30% of cases, depending on the population studied [66, 67]. This is unsurprising given that the two measurements describe different physiological processes—while FFR represents the effects of an epicardial stenosis on blood flow, MFR embodies information on both the epicardial and microvascular circulations. Varying contributions of focal epicardial disease, diffuse epicardial disease, and microvascular disease create the interrelation between FFR and MFR [28•, 66].When both FFR and MFR are within normal range, significant epicardial and microvascular disease are excluded. Conversely, when both FFR and MFR are decreased, the presence of hemodynamically significant epicardial disease is confirmed and could be accompanied by microvascular disease, diffuse epicardial disease, or both. In cases of severe microvascular disease and absence of significant epicardial disease, MFR will be abnormally low while FFR will be preserved. In contrast, the presence of a significant focal epicardial lesion without significant microvascular disease will result in reduced FFR while MFR can remain above the threshold defining normality. The latter scenario is more frequently seen in younger and "healthier" individuals and can be explained by the fact that MFR thresholds have typically been determined in populations with both microvascular and epicardial disease. Hence, in younger individuals without microvascular disease, utilization of these thresholds can underestimate the severity of epicardial lesions.

MBF in Cardiac Transplant Allograft Vasculopathy

Flow quantification with PET can also be used for a wide range of non-ischemic cardiomyopathies, an interesting example being CAV. CAV affects approximately one-third of cardiac transplant patients and is among the leading cause of graft failure, limiting long-term survival [68]. CAV is characterized by diffuse and concentric epicardial and microvasculature intimal thickening which contrasts with the focal and eccentric plaques typically seen in CAD [69]. Early detection of CAV is of critical importance for the timely initiation of therapy. However, diagnosis is complicated by the fact that signs and symptoms are non-specific, if not completely absent. Currently, the modality of choice to detect CAV is coronary angiography, with or without intravascular ultrasound (IVUS); however, the sensitivity of angiography is hampered by the diffuse, concentric, and longitudinal nature of the disease. Moreover, angiography is not well suited to assess microvasculature, which is often affected in CAV. Interestingly, CAV is associated with impaired coronary vasodilatory capacity, with the degree of impairment correlating with the severity of CAV [32]. Because of the diffuse nature of CAV, SPECT MPI is not very useful for detecting the impaired coronary vasodilatory capacity seen in this condition [70, 71]. On the other hand, MBF assessment with PET represents a useful assessment tool as it provides information on both epicardial (whether focal or diffuse) and microvascular involvement. In fact, it has been shown that abnormal quantitative measurements of MBF and MFR are associated with the presence of CAV on angiography and can predict disease progression and adverse events [72–74]. In a recent prospective study evaluating the role of ^{82}Rb-RbCl PET/CT MPI in heart transplant patients, flow measurements were shown to correlate with invasive coronary flow measures and had a high diagnostic accuracy in detecting CAV [75••]. The coronary vascular resistance (CVR) index, defined as systolic blood pressure divided by stress MBF, helped distinguish between epicardial and microvascular involvement, as an increased CVR index was associated with microvascular dysfunction. A combination of stress MBF, MFR, and CVR index provided the optimal diagnostic performance for the detection of CAV, superior to any parameter alone. Based on these results, a diagnostic algorithm allowing non-invasive screening of transplant patients was proposed in order to guide invasive testing with angiography [75••]. Importantly, resting hyperemia is frequently seen in the months following cardiac transplantation and can persist for 1 to 3 years following surgery [76]. This elevation in resting flows translates into a reduction of MFR which should not be mistaken for CAV [11••].

Conclusion

The first studies examining the use of myocardial flow quantification with PET date back to the 1960s. Since that time, technological advances and the availability of validated software packages have rendered this technique robust and reproducible to the point that PET is now considered the gold standard for non-invasive assessment of MBF. To date, numerous

studies have demonstrated the diagnostic and prognostic value of MBF quantification in CAD and various other conditions. Flow quantification enhances the ability of MPI to detect significant epicardial disease and can be useful in the assessment of coronary microvascular dysfunction in both ischemic and non-ischemic cardiomyopathies. Overall, MFR and MBF can lead to improved risk stratification by providing information complementary to that of other markers of disease severity, such as FFR.

Compliance with Ethical Standards

Conflict of Interest Matthieu Pelletier-Galarneau and Patrick Martineau declare that they have no conflict of interest.

Georges El Fakhri reports a patent issued that is titled Fast, Unique and Robust Factor Analysis (on estimation of Inout Function and Quantification of MBF) with royalties paid to INVIA, LLC.

Human and Animal Rights and Informed Consent This article does not contain any studies with human or animal subjects performed by any of the authors.

Publisher's Note Springer Nature remains neutral with regard to jurisdictional claims in published maps and institutional affiliations.

References

Papers of particular interest, published recently, have been highlighted as:
- • Of importance
- •• Of major importance

1. Ward RP, Al-Mallah MH, Grossman GB, Hansen CL, Hendel RC, Kerwin TC, et al. American Society of Nuclear Cardiology review of the ACCF/ASNC appropriateness criteria for single-photon emission computed tomography myocardial perfusion imaging (SPECT MPI). J Nucl Cardiol. 2007;14:e26–38.
2. Jaarsma C, Leiner T, Bekkers SC, Crijns HJ, Wildberger JE, Nagel E, et al. Diagnostic performance of noninvasive myocardial perfusion imaging using single-photon emission computed tomography, cardiac magnetic resonance, and positron emission tomography imaging for the detection of obstructive coronary artery disease: a meta-analysis. J Am Coll Cardiol. 2012;59:1719–28.
3. Shanoudy H, Raggi P, Beller GA, Soliman A, Ammermann EG, Kastner RJ, et al. Comparison of technetium-99m tetrofosmin and thallium-201 single-photon emission computed tomographic imaging for detection of myocardial perfusion defects in patients with coronary artery disease. J Am Coll Cardiol. 1998;31:331–7.
4. Burrell S, MacDonald A. Artifacts and pitfalls in myocardial perfusion imaging. J Nucl Med Technol. 2006;34:193–211.
5. Lima RSL, Watson DD, Goode AR, Siadaty MS, Ragosta M, Beller GA, et al. Incremental value of combined perfusion and function over perfusion alone by gated SPECT myocardial perfusion imaging for detection of severe three-vessel coronary artery disease. J Am Coll Cardiol. 2003;42:64–70.
6. Bing RJ, Bennish A, Bluemchen G, Cohen A, Gallagher JP, Zaleski EJ. Determination of coronary flow equivalent with coincidence counting technic. Circulation. 1964;29:833–46.
7. RUBY-FILL® (Rubidium Rb82 Generator) [package insert]. Jubilant DRAXIMAGE Inc., Kirkland, Québec, Canada. 2016.
8. Ghotbi AA, Kjær A, Hasbak P. Review: comparison of PET rubidium-82 with conventional SPECT myocardial perfusion imaging. Clin Physiol Funct Imaging. 2014;34:163–70.
9. Dilsizian V, Taillefer R. Journey in evolution of nuclear cardiology: will there be another quantum leap with the F-18-labeled myocardial perfusion tracers? JACC Cardiovasc Imaging. 2012;5:1269–84.
10. Sherif HM, Nekolla SG, Saraste A, Reder S, Yu M, Robinson S, et al. Simplified quantification of myocardial flow reserve with flurpiridaz F 18: validation with microspheres in a pig model. J Nucl Med. 2011;52:617–24.
11. •• Murthy VL, Bateman TM, Beanlands RS, Berman DS, Borges-Neto S, Chareonthaitawee P, et al. Clinical quantification of myocardial blood flow using PET: joint position paper of the SNMMI cardiovascular council and the ASNC. J Nucl Med. 2018;59:273–93. **Recent joint position paper of the SNMMI and ASNC with extensive and critical literature review as well as procedural recommendations for PET MPI and MBF quantification.**
12. •• Dilsizian V, Bacharach SL, Beanlands RS, Bergmann SR, Delbeke D, Dorbala S, et al. ASNC imaging guidelines/SNMMI procedure standard for positron emission tomography (PET) nuclear cardiology procedures. J Nucl Cardiol. 2016;23:1187–226. **Joint position paper of the SNMMI and ASNC with extensive and critical literature review as well as procedural recommendations for PET quality control.**
13. Dekemp RA, Declerck J, Klein R, Pan X-B, Nakazato R, Tonge C, et al. Multisoftware reproducibility study of stress and rest myocardial blood flow assessed with 3D dynamic PET/CT and a 1-tissue-compartment model of 82Rb kinetics. J Nucl Med. 2013;54:571–7.
14. Alpert N, Dean Fang Y-H, Fakhri GE. Single-scan rest/stress imaging 18F-labeled flow tracers. Med Phys. 2012;39:6609–20.
15. Guehl NJ, Normandin MD, Wooten DW, Rozen G, Ruskin JN, Shoup TM, et al. Rapid computation of single PET scan rest-stress myocardial blood flow parametric images by table look up. Med Phys. 2017;44:4643–51.
16. • Guehl NJ, Normandin MD, Wooten DW, Rozen G, Sitek A, Ruskin J, et al. Single-scan rest/stress imaging: validation in a porcine model with 18F-Flurpiridaz. Eur J Nucl Med Mol Imaging. 2017;44:1538–46. **This paper validates a shortened PET MPI protocol with flurpiridaz. With the proposed protocol, both rest and stress acquisitions can be obtained within less than 15 min and during a single scan.**
17. Pelletier-Galarneau M, Guehl N, Kim SJW, Osborne M, Radfar A, Normandin M, et al. Two-injection single-scan rest/stress imaging with 13N-ammonia: first human studies. J Nucl Med. 2018;59:1515.
18. Gonzalez JA, Beller GA. Choosing exercise or pharmacologic stress imaging, or exercise ECG testing alone: how to decide. J Nucl Cardiol. 2017;24:555–7.
19. Valenta I, Quercioli A, Vincenti G, Nkoulou R, Dewarrat S, Rager O, et al. Structural epicardial disease and microvascular function are determinants of an abnormal longitudinal myocardial blood flow difference in cardiovascular risk individuals as determined with PET/CT. J Nucl Cardiol. 2010;17:1023–33.
20. Johnson NP, Gould KL. Integrating noninvasive absolute flow, coronary flow reserve, and ischemic thresholds into a comprehensive map of physiological severity. JACC Cardiovasc Imaging. 2012;5:430–40.
21. Lortie M, Beanlands RSB, Yoshinaga K, Klein R, Dasilva JN, DeKemp RA. Quantification of myocardial blood flow with 82Rb dynamic PET imaging. Eur J Nucl Med Mol Imaging. 2007;34:1765–74.
22. Prior JO, Schindler TH, Facta AD, Hernandez-Pampaloni M, Campisi R, Dahlbom M, et al. Determinants of myocardial blood

flow response to cold pressor testing and pharmacologic vasodilation in healthy humans. Eur J Nucl Med Mol Imaging. 2007;34:20–7.
23. Aquaro GD, Todiere G, Barison A, Strata E, Marzilli M, Pingitore A, et al. Myocardial blood flow and fibrosis in hypertrophic cardiomyopathy. J Card Fail. 2011;17:384–91.
24. Czernin J, Müller P, Chan S, Brunken RC, Porenta G, Krivokapich J, et al. Influence of age and hemodynamics on myocardial blood flow and flow reserve. Circulation. 1993;88:62–9.
25. Motivala AA, Rose PA, Kim HM, Smith YR, Bartnik C, Brook RD, et al. Cardiovascular risk, obesity, and myocardial blood flow in postmenopausal women. J Nucl Cardiol. 2008;15:510–7.
26. Tawakol A, Sims K, MacRae C, Friedman JR, Alpert NM, Fischman AJ, et al. Myocardial flow regulation in people with mitochondrial myopathy, encephalopathy, lactic acidosis, stroke-like episodes/myoclonic epilepsy and ragged red fibers and other mitochondrial syndromes. Coron Artery Dis. 2003;14:197–205.
27. Ramanathan T, Skinner H. Coronary blood flow. Contin Educ Anaesth Crit Care Pain. 2005;5:61–4.
28.• Gewirtz H. Coronary circulation: pressure/flow parameters for assessment of ischemic heart disease. J Nucl Cardiol. 2018. https://doi.org/10.1007/s12350-018-1270-3. **This paper is an elegant review of the physiological principles behind flow measurements with different modalities, allowing a better understanding of those parameters.**
29. Pelletier-Galarneau M, deKemp RA, Hunter CRRN, Klein R, Klein M, Ironstone J, et al. Effects of hypercapnia on myocardial blood flow in healthy human subjects. J Nucl Med. 2018;59:100–6.
30. Germino M, Ropchan J, Mulnix T, Fontaine K, Nabulsi N, Ackah E, et al. Quantification of myocardial blood flow with (82)Rb: validation with (15)O-water using time-of-flight and point-spread-function modeling. EJNMMI Res. 2016;6:68.
31. Tadamura E, Iida H, Matsumoto K, Mamede M, Kubo S, Toyoda H, et al. Comparison of myocardial blood flow during dobutamine-atropine infusion with that after dipyridamole administration in normal men. J Am Coll Cardiol. 2001;37:130–6.
32. Kofoed KF, Czernin J, Johnson J, Kobashigawa J, Phelps ME, Laks H, et al. Effects of cardiac allograft vasculopathy on myocardial blood flow, vasodilatory capacity, and coronary vasomotion. Circulation. 1997;95:600–6.
33. Hajjiri MM, Leavitt MB, Zheng H, Spooner AE, Fischman AJ, Gewirtz H. Comparison of positron emission tomography measurement of adenosine-stimulated absolute myocardial blood flow versus relative myocardial tracer content for physiological assessment of coronary artery stenosis severity and location. JACC Cardiovasc Imaging. 2009;2:751–8.
34. Fiechter M, Ghadri JR, Gebhard C, Fuchs TA, Pazhenkottil AP, Nkoulou RN, et al. Diagnostic value of 13N-ammonia myocardial perfusion PET: added value of myocardial flow reserve. J Nucl Med. 2012;53:1230–4.
35. Muzik O, Duvernoy C, Beanlands RS, Sawada S, Dayanikli F, Wolfe ER, et al. Assessment of diagnostic performance of quantitative flow measurements in normal subjects and patients with angiographically documented coronary artery disease by means of nitrogen-13 ammonia and positron emission tomography. J Am Coll Cardiol. 1998;31:534–40.
36. Ziadi MC, Dekemp RA, Williams K, Guo A, Renaud JM, Chow BJW, et al. Does quantification of myocardial flow reserve using rubidium-82 positron emission tomography facilitate detection of multivessel coronary artery disease? J Nucl Cardiol. 2012;19:670–80.
37. Naya M, Murthy VL, Taqueti VR, Foster CR, Klein J, Garber M, et al. Preserved coronary flow reserve effectively excludes high-risk coronary artery disease on angiography. J Nucl Med. 2014;55:248–55.
38. Danad I, Uusitalo V, Kero T, Saraste A, Raijmakers PG, Lammertsma AA, et al. Quantitative assessment of myocardial perfusion in the detection of significant coronary artery disease: cutoff values and diagnostic accuracy of quantitative [(15)O]H2O PET imaging. J Am Coll Cardiol. 2014;64:1464–75.
39. Danad I, Raijmakers PG, Harms HJ, Heymans MW, van Royen N, Lubberink M, et al. Impact of anatomical and functional severity of coronary atherosclerotic plaques on the transmural perfusion gradient: a [15O]H2O PET study. Eur Heart J. 2014;35:2094–105.
40. Joutsiniemi E, Saraste A, Pietilä M, Mäki M, Kajander S, Ukkonen H, et al. Absolute flow or myocardial flow reserve for the detection of significant coronary artery disease? Eur Heart J Cardiovasc Imaging. 2014;15:659–65.
41. Lee JM, Kim CH, Koo B-K, Hwang D, Park J, Zhang J, et al. Integrated myocardial perfusion imaging diagnostics improve detection of functionally significant coronary artery stenosis by 13N-ammonia positron emission tomography. Circ Cardiovasc Imaging. 2016;9:e004768.
42. Williams MC, Mirsadraee S, Dweck MR, Weir NW, Fletcher A, Lucatelli C, et al. Computed tomography myocardial perfusion vs 15O-water positron emission tomography and fractional flow reserve. Eur Radiol. 2017;27:1114–24.
43. Stuijfzand WJ, Uusitalo V, Kero T, Danad I, Rijnierse MT, Saraste A, et al. Relative flow reserve derived from quantitative perfusion imaging may not outperform stress myocardial blood flow for identification of hemodynamically significant coronary artery disease. Circ Cardiovasc Imaging. 2015;8:e002400.
44. Danad I, Raijmakers PG, Appelman YE, Harms HJ, de Haan S, van den Oever MLP, et al. Hybrid imaging using quantitative H215O PET and CT-based coronary angiography for the detection of coronary artery disease. J Nucl Med. 2013;54:55–63.
45. Murthy VL, Naya M, Foster CR, Hainer J, Gaber M, Di Carli G, et al. Improved cardiac risk assessment with noninvasive measures of coronary flow reserve. Circulation. 2011;124:2215–24.
46. Ziadi MC, Dekemp RA, Williams KA, Guo A, Chow BJW, Renaud JM, et al. Impaired myocardial flow reserve on rubidium-82 positron emission tomography imaging predicts adverse outcomes in patients assessed for myocardial ischemia. J Am Coll Cardiol. 2011;58:740–8.
47. Johnson NP, Gould KL. Physiological basis for angina and ST-segment change PET-verified thresholds of quantitative stress myocardial perfusion and coronary flow reserve. JACC Cardiovasc Imaging. 2011;4:990–8.
48. Tio RA, Dabeshlim A, Siebelink H-MJ, de Sutter J, Hillege HL, Zeebregts CJ, et al. Comparison between the prognostic value of left ventricular function and myocardial perfusion reserve in patients with ischemic heart disease. J Nucl Med. 2009;50:214–9.
49. Slart RHJA, Zeebregts CJ, Hillege HL, de Sutter J, Dierckx RAJO, van Veldhuisen DJ, et al. Myocardial perfusion reserve after a PET-driven revascularization procedure: a strong prognostic factor. J Nucl Med. 2011;52:873–9.
50. Herzog BA, Husmann L, Valenta I, Gaemperli O, Siegrist PT, Tay FM, et al. Long-term prognostic value of 13N-ammonia myocardial perfusion positron emission tomography added value of coronary flow reserve. J Am Coll Cardiol. 2009;54:150–6.
51. Murthy VL, Naya M, Foster CR, Gaber M, Hainer J, Klein J, et al. Association between coronary vascular dysfunction and cardiac mortality in patients with and without diabetes mellitus. Circulation. 2012;126:1858–68.
52. Murthy VL, Naya M, Foster CR, Hainer J, Gaber M, Dorbala S, et al. Coronary vascular dysfunction and prognosis in patients with chronic kidney disease. JACC Cardiovasc Imaging. 2012;5:1025–34.
53.• Shah NR, Charytan DM, Murthy VL, Skali Lami H, Veeranna V, Cheezum MK, et al. Prognostic value of coronary flow reserve in patients with dialysis-dependent ESRD. J Am Soc Nephrol JASN.

2016;27:1823–9. **This study shows the independent and incremental value of MFR for risk stratification of patients with end-stage renal disease.**

54. Dorbala S, Vangala D, Bruyere J, Quarta C, Kruger J, Padera R, et al. Coronary microvascular dysfunction is related to abnormalities in myocardial structure and function in cardiac amyloidosis. JACC Heart Fail. 2014;2:358–67.
55. Kalliokoski RJ, Kalliokoski KK, Sundell J, Engblom E, Penttinen M, Kantola I, et al. Impaired myocardial perfusion reserve but preserved peripheral endothelial function in patients with Fabry disease. J Inherit Metab Dis. 2005;28:563–73.
56. Neglia D, Michelassi C, Trivieri MG, Sambuceti G, Giorgetti A, Pratali L, et al. Prognostic role of myocardial blood flow impairment in idiopathic left ventricular dysfunction. Circulation. 2002;105:186–93.
57. Sciagrà R, Calabretta R, Cipollini F, Passeri A, Castello A, Cecchi F, et al. Myocardial blood flow and left ventricular functional reserve in hypertrophic cardiomyopathy: a 13NH3 gated PET study. Eur J Nucl Med Mol Imaging. 2017;44:866–75.
58. Majmudar MD, Murthy VL, Shah RV, Kolli S, Mousavi N, Foster CR, et al. Quantification of coronary flow reserve in patients with ischaemic and non-ischaemic cardiomyopathy and its association with clinical outcomes. Eur Heart J Cardiovasc Imaging. 2015;16:900–9.
59. Kajander S, Joutsiniemi E, Saraste M, Pietilä M, Ukkonen H, Saraste A, et al. Cardiac positron emission tomography/computed tomography imaging accurately detects anatomically and functionally significant coronary artery disease. Circulation. 2010;122:603–13.
60. Gewirtz H, Dilsizian V. Integration of quantitative positron emission tomography absolute myocardial blood flow measurements in the clinical management of coronary artery disease. Circulation. 2016;133:2180–96.
61. Juneau D, Erthal F, Ohira H, Mc Ardle B, Hessian R, Beanlands RS, et al. Clinical PET myocardial perfusion imaging and flow quantification. Cardiol Clin. 2016;34:69–85.
62. Juneau D, deKemp RA, Beanlands RSB. Reporting myocardial flow reserve with PET. Ready or not, here it is! But walk before you fly! J Nucl Cardiol. 2018;25:164–8.
63. Xaplanteris P, Fournier S, Pijls NHJ, Fearon WF, Barbato E, Tonino PAL, et al. Five-year outcomes with PCI guided by fractional flow reserve. N Engl J Med. 2018;379:250–9.
64. De Bruyne B, Pijls NHJ, Kalesan B, Barbato E, Tonino PAL, Piroth Z, et al. Fractional flow reserve-guided PCI versus medical therapy in stable coronary disease. N Engl J Med. 2012;367:991–1001.
65. De Bruyne B, Fearon WF, Pijls NHJ, Barbato E, Tonino P, Piroth Z, et al. Fractional flow reserve-guided PCI for stable coronary artery disease. N Engl J Med. 2014;371:1208–17.
66. Johnson NP, Kirkeeide RL, Gould KL. Is discordance of coronary flow reserve and fractional flow reserve due to methodology or clinically relevant coronary pathophysiology? JACC Cardiovasc Imaging. 2012;5:193–202.
67. Meimoun P, Sayah S, Luycx-Bore A, Boulanger J, Elmkies F, Benali T, et al. Comparison between non-invasive coronary flow reserve and fractional flow reserve to assess the functional significance of left anterior descending artery stenosis of intermediate severity. J Am Soc Echocardiogr. 2011;24:374–81.
68. Lund LH, Edwards LB, Dipchand AI, Goldfarb S, Kucheryavaya AY, Levvey BJ, et al. The registry of the International Society for Heart and Lung Transplantation: thirty-third adult heart transplantation report-2016; focus theme: primary diagnostic indications for transplant. J Heart Lung Transplant. 2016;35:1158–69.
69. Ramzy D, Rao V, Brahm J, Miriuka S, et al. Cardiac allograft vasculopathy: a review. Can J Surg. 2005;48:319.
70. Thompson D, Koster MJ, Wagner RH, Heroux A, Barron JT. Single photon emission computed tomography myocardial perfusion imaging to detect cardiac allograft vasculopathy. Eur Heart J Cardiovasc Imaging. 2012;13:271–5.
71. Manrique A, Bernard M, Hitzel A, Bubenheim M, Tron C, Agostini D, et al. Diagnostic and prognostic value of myocardial perfusion gated SPECT in orthotopic heart transplant recipients. J Nucl Cardiol. 2010;17:197–206.
72. Wu Y-W, Chen Y-H, Wang S-S, Jui H-Y, Yen R-F, Tzen K-Y, et al. PET assessment of myocardial perfusion reserve inversely correlates with intravascular ultrasound findings in angiographically normal cardiac transplant recipients. J Nucl Med. 2010;51:906–12.
73. Allen-Auerbach M, Schöder H, Johnson J, Kofoed K, Einhorn K, Phelps ME, et al. Relationship between coronary function by positron emission tomography and temporal changes in morphology by intravascular ultrasound (IVUS) in transplant recipients. J Heart Lung Transplant. 1999;18:211–9.
74. Mc Ardle BA, Davies RA, Chen L, Small GR, Ruddy TDR, Dwivedi G, et al. The prognostic value of Rb-82 positron emission tomography in patients following heart transplant. Circ Cardiovasc Imaging. 2014;7:930–7.
75.•• Chih S, Chong AY, Erthal F, de Kemp RA, Davies RA, Stadnick E, et al. PET assessment of epicardial intimal disease and microvascular dysfunction in cardiac allograft vasculopathy. J Am Coll Cardiol. 2018;71:1444–56. **This recent prospective study showed that flow quantification with PET can diagnose CAV with high accuracy. The authors also proposed an investigation algorithm which uses PET flow quantification as a potential tool for non-invasive screening of CAV.**
76. Kushwaha SS, Narula J, Narula N, Zervos G, Semigran MJ, Fischman AJ, et al. Pattern of changes over time in myocardial blood flow and microvascular dilator capacity in patients with normally functioning cardiac allografts. Am J Cardiol. 1998;82:1377–81.